Centrum voor Wiskunde en Informatica
Centre for Mathematics and Computer Science

H.A. Lauwerier, M.B. van der Mark

Chaos and order in an optical ring cavity

Department of Applied Mathematics Report AM-R8416 November

Bibliotheek
Centrum voor Wiskunde en Informatica
Amsterdam

The Centre for Mathematics and Computer Science is a research institute of the Stichting Mathematisch Centrum, which was founded on February 11, 1946, as a nonprofit institution aiming at the promotion of mathematics, computer science, and their applications. It is sponsored by the Dutch Government through the Netherlands Organization for the Advancement of Pure Research (Z.W.O.).

Copyright © Stichting Mathematisch Centrum, Amsterdam

CHAOS AND ORDER IN AN OPTICAL RING CAVITY

H.A. LAUWERIER
Centre for Mathematics and Computer Science, Amsterdam

M.B. VAN DER MARK
Natuurkundig Laboratorium, Universiteit van Amsterdam

This study originates from an attempt to understand the bifurcation behaviour in a certain two-dimensional iterative map considered by Ikeda et al. in a theoretical study of optical bistability. The map can be written in complex coordinates z and $\bar{z}$ in the following form: $z' = A + Bz \exp i(z\bar{z} - \beta)$.
The complex coordinate z has the meaning of an electric field vector, A is the amplitude of the incoming wave, B measures the dissipation of the electric energy and β is called a mistuning parameter. The mapping is considered from a mathematical point of view, by using the usual techniques of two-dimensional maps. The parameter B determines whether the map is Hamiltonian ($B = 1$), i.e. measure preserving, or dissipative ($B < 1$). Various plots are given showing the chaotic behaviour of the map, periodic points, continuous invariant curves, isolated structures, strange attractors, etc.

1980 MATHEMATICS SUBJECT CLASSIFICATION: 58F14, 58F13, 78A10.
KEY WORDS & PHRASES: iterative maps, chaotic behaviour, strange attractor.
NOTE: This report will be submitted for publication elsewhere.

Report AM-R8416
Centre for Mathematics and Computer Science
P.O. Box 4079, 1009 AB Amsterdam, The Netherlands

Introduction

This study originates from an attempt to understand the bifurcation behaviour in a certain two-dimensional iterative map considered by Ikeda et al. [1] in a theoretical study of optical turbulence. The map can be written in complex coordinates z and $\bar{z}$ in the form

$$z' = A + Bz \exp i(z\bar{z} - \beta), \tag{1.1}$$

which may be converted to real form either in Cartesian coordinates or in polar coordinates by using

$$z = x + iy, \qquad \bar{z} = x - iy, \tag{1.2}$$

or

$$z = r \exp i\theta, \qquad \bar{z} = r \exp -i\theta. \tag{1.3}$$

For the physical interpretation of (1.1) we refer to the paper quoted above. The complex coordinate z has the meaning of an electric field vector, A is the amplitude of the incoming wave, B measures the dissipation of the electric energy and β is called a mistuning parameter. In the paper an intriguing plot was given of a series of 5000 successsive points of the map (1.1) for the parameter values $A = 3.9$, $B = 0.4$ and $\beta = 0$. Shown is what looks like a strange attractor. A similar illustration is given here in Fig.4.1 and 4.2 for $A = 2$, $B = 0.6$ and $\beta = 0$. In Section 4 it is shown that these points are also attracted by the unstable manifold of an unstable fixed point. An initial section of such an invariant curve given in parameter form by analytic functions is shown in Fig.4.3 for the conditions of Fig.4.1.

In this paper the map (1.1) will be studied from a mathematician point of view using the usual techniques for two-dimensional maps. As a rule the parameters are restricted to the following ranges.

$$A > 0, \qquad 0 < B \leqslant 1, \qquad 0 \leqslant \beta < 2\pi \tag{1.4}$$

However, in some cases it might be desirable to give A also negative values, but then β can be restricted to the interval $(0,\pi)$. The map (1.1) can be considered as a combination of a rotation, a similarity transformation and a translation. If R denotes the combined effect of a rotation and a reduction of scale by the factor B

$$R \quad \begin{cases} r' = Br \\ \theta' = r^2 - \beta, \end{cases} \tag{1.5}$$

and T the translation

$$T \quad \begin{cases} x' = x + A, \\ y' = y, \end{cases} \tag{1.6}$$

then the map (1.1) can be written as TR i.e. R followed by T. Obviously the map is area-preserving for $B = 1$ and area-contracting for $B < 1$. The dissipative case $B < 1$ and the Hamiltonian case $B = 1$ behave quite differently as is well-known. In the dissipative case we may have one or more (locally) stable fixed points. A typical plot is shown in Fig.1.1 for $A = 0.5$, $B = 0.99$, $\beta = 0$. All points are attracted towards the single stable fixed point at $x = 0.2625$, $y = 0.7552$. In Section 2 the dissipative case $B < 1$ is studied in detail. All fixed points are situated on an Apollonius circle with respect to $z = 0$ and $z = A$. Formulas are given for determining their position, (2.4) and (2.6), and their possible stability (2.12), (2.16) and (2.17). The conditions for stability are given a geometrical interpretation in Fig.2.3 and Fig.2.5 so that e.g. for a fixed value of B and arbitrary values of A and β the possible stability of a particular fixed point can be read off at once. In striking contrast to this is the Hamiltonian case. A typical illustration is Fig.1.2 for $A = 0.5$, $B = 1$, $\beta = 0$ in which 6 orbits are given, around the fixed point at $x = 0.25$, $y = 0.7580$. This map shows all the familiar phenomena such as periodic points, continuous invariant curves, chaotic rings and island structures.

In Section 3 the Hamiltonian case is considered in detail as regards the positions of the fixed points and their nature. All fixed points are on the line $x = A/2$ and this line is a line of symmetry of the Hamiltonian map.

In Section 4 we consider the pseudo-chaotic case when all fixed points of the dissipative map are

unstable. It is shown that the attractor is always contained in the closed disk $|z-A| \leqslant AB/(1-B)$. An explicit construction is given of the unstable manifold of an unstable fixed point. It can be represented in complex form by

$$z = z_0 + \sum_{k=1}^{\infty} c_k t^k$$

where t is a real parameter. The action of the map (1.1) on the unstable manifold is simply $t \to \lambda t$ where λ is the unstable multiplier ($|\lambda| > 1$) of the fixed point z_0. This enables us to find expressions for the first few coefficients c_k. Once a small initial arc of the invariant manifold departing from z_0 is known it can be continued almost indefinitely along the invariant curve. The idea is that the "strange" attractor is the limit set of the unstable invariant curve. Since this curve appears to be folded up upon itself infinitely often it is itself a convincing continuous representative of the still somewhat mysterious "strange" attractor. It is of interest to compare Fig.4.1 and Fig.4.3 as the discrete and the continuous representation of the same object.

2. The dissipative case

A fixed point of (1.1) is determined by the relation

$$z = A + Bz \exp i(r^2 - \beta). \tag{2.1}$$

This gives

$$|(z-A)/z| = B, \tag{2.2}$$

and

$$|1 - B \exp i(r^2-\beta)| = \frac{A}{r}. \tag{2.3}$$

The relation (2.2) says that fixed points are situated on a so-called Appollonius circle for which $z=0$ and $z=A$ are conjugate points. Its centre is $z = A/(1-B^2)$ and its radius equals $AB/(1-B^2)$ (cf. Fig.2.1).

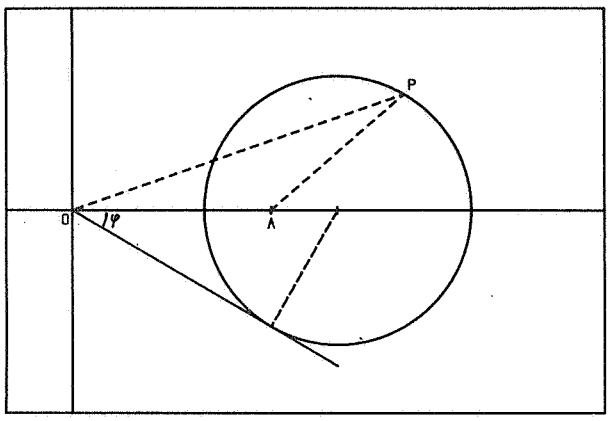

Fig. 2.1. Apollonius' circle: $AP/OP = B$.

It is inside and tangent to the sector $-\phi \leqslant \theta \leqslant \phi$ with $\sin\phi = B$. The second relation (2.3) written in real form as

$$1 - 2B\cos(r^2-\beta) + B^2 = \frac{A^2}{r^2}. \tag{2.4}$$

This equation gives the r-coordinates of the fixed points. They can be obtained graphically as shown in Fig.2.2 by plotting each side of (2.4) as a function of r^2 in the same graph. In order to compute the positions r, θ of the fixed points we may use the relations (2.2) and (2.4) or any equivalent relations such

as

$$\begin{cases} B\cos(r^2-\beta) = 1-\dfrac{A}{r}\cos\theta, \\ B\sin(r^2-\beta) = \dfrac{A}{r}\sin\theta \end{cases} \tag{2.5}$$

which can easily be obtained from (2.1). The first step is the determination of r^2 from (2.4) guided by a graph as Fig.2.2. The next step is finding θ using

$$\theta = \arcsin\left(\frac{Br}{A}\sin(r^2-\beta)\right). \tag{2.6}$$

For $A=1$, $B=0.6$ and $\beta=0$ we find

$$r^2 = 1.15, \quad \theta = 0.63, \quad x = 0.87, \quad y = 0.63.$$

For $A=2$ we obtain with the same values of B and β the following set of fixed points.

r^2	r	θ	x	y	β
2.07	1.44	0.39	1.33	0.55	1.19
5.23	2.29	-0.64	1.84	-1.36	-1.01
7.13	2.67	0.64	2.14	1.60	1.90
12.02	3.47	-0.57	2.92	-1.86	-1.62
13.07	3.61	0.55	3.09	1.87	2.11
18.54	4.31	-0.40	3.97	-1.68	-1.46
19.14	4.37	0.38	4.06	1.62	1.84

Table 2.1

The meaning of the parameter β, the degree of (in)stability will be explained below.

In order to analyze the possible stability of a particular fixed point we need its multipliers λ_1 and λ_2. Since areas are contracted by the factor B^2 we know already that

$$\lambda_1\lambda_2 = B^2. \tag{2.7}$$

For the trace $\lambda_1+\lambda_2$ we use the following expression holding for a complex map $z'=z'(z,\bar{z})$

$$\lambda_1+\lambda_2 = 2\,\mathrm{Re}\frac{\partial z'}{\partial z} \tag{2.8}$$

A simple calculation shows that

$$\tfrac{1}{2}(\lambda_1+\lambda_2) = B(\cos(r^2-\beta)-r^2\sin(r^2-\beta)) \tag{2.9}$$

Using the expression (2.5) we may write

$$\tfrac{1}{2}(\lambda_1+\lambda_2) = 1-A\,/\,r(\cos\theta+r^2\sin\theta). \tag{2.10}$$

The condition for stability is that both multipliers are inside the unit circle. An equivalent condition is

$$|\lambda_1+\lambda_2| < 1+\lambda_1\lambda_2. \tag{2.11}$$

Substitution of the expressions (2.7) and 2.10 gives

$$\frac{1-B^2}{2A} < \frac{1}{r}\cos\theta+r\sin\theta < \frac{3+B^2}{2A}. \tag{2.12}$$

For each fixed point obtained from (2.4) and (2.6) this condition can be checked by considering the value of the so-called parameter of (in)stability

$$p = \frac{1}{r}\cos\theta+r\sin\theta. \tag{2.13}$$

E.g. for $A=2$, $B=0.6$, $\beta=0$ the values of c are given in Table 2.1. The boundaries of the stability interval are 0.16 and 0.84. This shows that all fixed points are unstable. In order to do this in a more general way we have plotted in Fig.2.3 a number of curves defined by (2.13) for a few values of p. Then at least for $A>1$ and $0<B\leqslant 1$ the possible stability of a fixed point can be read off at once.

One may ask the following question. Are there regions in the x,y-plane where fixed points are always stable or unstable? In all its generality this is asking too much since there are three free parameters A, B and β. However, if B is given a fixed value and A and β are considered as arbitrary then the question can be answered in an affirmative way.

Let P_0 be a given fixed point with coordinates x_0,y_0 or r_0,θ_0 then values of A and β can be derived as follows. We know that P_0 is on an Apollonius circle for some A and that this circle is tangent to the lines $\theta=\pm\arcsin B$. This shows that for a given value of B only points with $|\sin\theta_0|\leqslant B$ can be fixed points. The Apollonius circle can be determined by means of a nice geometrical construction as shown in Fig.2.4. The problem is essentially the determination of a circle passing through two given points P_0 and Q_0, the mirror image of P_0, and a given line, say $\theta=\arcsin B$. The geometrical construction is determined by the property $ST_1=ST_2=\sqrt{SP_0.SQ_0}$. There are two solutions. If A_1 and A_2 are the projection of the tangent points T_1 and T_2 on the x-axis we see that $\frac{1}{2}(x(A_1)+x(A_2))=x_0$.

The value of A can be obtained from (2.2) by solving the quadratic equation (2.14) $A^2-2Ar_0\cos\theta_0+(1-B^2)r_0^2=0$.

We obtain the two values, dropping the subscripts,

$$\begin{cases} A_1 = r(\cos\theta-\sqrt{B^2-\sin^2\theta}), \\ A_2 = r(\cos\theta+\sqrt{B^2-\sin^2\theta}). \end{cases} \tag{2.15}$$

A simple observation in Fig.2.4 shows that these values are the x-coordinates of A_2 and A_1. The corresponding value of β is determined from (2.1) as

$$\beta = r^2+arg\frac{z}{z-A} \quad (mod\ 2\pi), \tag{2.16}$$

or (cf. Fig. 2.1)

$$\beta = r^2-\angle\ OPA.$$

If the values of (2.15) are substituted in (2.12) we find after a few elementary calculations the following stability conditions:

Case A_1

$$\begin{cases} \text{for } \theta\geqslant 0 & 2r^2\sin\theta < C\cos\theta+(C+2)\sqrt{B^2-\sin^2\theta} \\ \text{for } \theta<0 & 2r^2|\sin\theta| < \cos\theta-\sqrt{B^2-\sin^2\theta} \end{cases} \tag{2.17}$$

Case A_2

$$\begin{cases} \text{for } \theta>0 & 2r^2\sin\theta < C\cos\theta-(C+2)\sqrt{B^2-\sin^2\theta} \\ \text{for } \theta\leqslant 0 & 2r^2|\sin\theta| < \cos\theta+\sqrt{B^2-\sin^2\theta} \end{cases} \tag{2.18}$$

where

$$C = \frac{3B^2+1}{1-B^2}. \tag{2.19}$$

In Fig.2.5 a geometric interpretation of these inequalities is given in a somewhat schematic way. In both upper and lower halfplane the region of stability are bounded by a curve which looks like a vertically compressed horizontal parabole tangent to the lines $\theta=\pm\arcsin B$.

In the notation of Fig.2.5 in I the fixed point is stable in both situations A_1 and A_2. In II there is stability only in the A_1 situation whereas in III both cases are unstable. In IV there is stability only in the A_2 situation whereas in IV there is always instability. In particular any fixed point on the real axis is always stable, a result that can be obtained also from (2.12) by taking $\theta=0$ and $A=r(1\pm B)$.

In Fig.2.6 the regions of full and partial stability are given for a few values of B. It appears that the boundaries are very sensitive to small changes in B if B is close to 1. This can be explained by the following asymptotic analysis. If $\epsilon=1-B$ is a small positive quantity we have in the lowest order ot approximation

$$\begin{cases} A_1 \approx \dfrac{\epsilon r}{\cos\theta} \\ A_2 \approx 2r\cos\theta - \dfrac{\epsilon r}{\cos\theta} \end{cases} \tag{2.20}$$

and

$$A_1 \begin{cases} \text{for } \theta \geqslant 0 & r^2 \sin\theta < \dfrac{2\cos\theta}{\epsilon} \\ \text{for } \theta < 0 & r^2 |\sin\theta| < \dfrac{\epsilon}{2\cos\theta} \end{cases} \tag{2.21}$$

$$A_2 \begin{cases} \text{for } \theta \geqslant 0 & r^2 < \tan\theta + \dfrac{\epsilon\tan\theta}{2\cos^2\theta} \\ \text{for } \theta < 0 & r^2 |\sin\theta| < \cos\theta - \dfrac{\epsilon}{2\cos\theta} \end{cases} \tag{2.22}$$

The conservative case $B=1$ for which $\epsilon=0$ will be considered in the next section.

3. The Hamiltonian case

The fixed points of the map with $B=1$ which is now Hamiltonian and area-preserving

$$z' = A + z\exp i(r^2-\beta) \tag{3.1}$$

follow from

$$z - A = z\exp i(r^2-\beta). \tag{3.2}$$

The relation

$$(z-A) = |z| \tag{3.3}$$

shows at once that all fixed points are on the line $x=\frac{1}{2}A$. It can be shown that this line is a line of symmetry for (3.1). This follows from the fact that (3.1) can be written as the product MS of two symmetric maps with

$$S: z' = \bar{z}\exp i(r^2-\beta),$$

and

$$M: z' = Z - \bar{z}.$$

The relation (3.2) can be written as

$$iA = r\exp i(\theta + \tfrac{1}{2}(r^2-\beta))\sin\tfrac{1}{2}(r^2-\beta).$$

Taking arguments we obtain

$$\theta = -\tfrac{1}{2}(r^2-\beta)+\tfrac{1}{2}\pi \quad (mod\ \pi). \tag{3.4}$$

Geometrically this says that the fixed points are the intersections of the two spirals

$$r = \sqrt{\beta+\pi-2\theta}\,, \quad r = \sqrt{\beta-\pi-2\theta} \tag{3.5}$$

with the vertical line $x = \frac{1}{2}A$. In (3.5) the argument θ should be taken as a continuously decreasing variable starting from $\theta = \frac{1}{2}(\beta\pm\pi)$. In Fig. 3.1 the situation is given for $\beta=0$ Obviously there is an infinity of fixed points. They can be enumerated by writing

$$r_k^2 = \beta-2\theta+(2k-1)\pi, \quad k = 0,1,2,... \tag{3.6}$$

where now θ is restricted to $(-\frac{1}{2}\pi,\frac{1}{2}\pi)$.

The condition of stability can be obtained from (2.12) by taking $B=1$. This gives

$$0 < A\,/\,r(\cos\theta+r^2\sin\theta) < 2. \tag{3.7}$$

The left-hand side can be reduced to

$$r^2\tan\theta > -1, \tag{3.8}$$

or

$$(x^2+y^2)y+x > 0$$

in Cartesian coordinates.

The geometrical interpretation of this condition is given in fig. 3.2. The right-hand side of (3.7) can be written as

$$\cos\theta(\cos\theta+r^2\sin\theta) < 1$$

since $A = 2x = 2r\cos\theta$. A little trigonometry gives

$$r\cot\theta < 1, \tag{3.9}$$

or

$$r^2\tan(\theta+\frac{\pi}{2}) > -1.$$

Thus we obtain a similar region as for (3.8) but with a quarter turn. The corresponding region is given in fig. 3.2 which combines both (3.8) and (3.9). We note that both conditions (3.8) and (3.9) follow as limit cases of (2.21). From the beginning it has been supposed that $A>0$ since this is sufficiently general. However, if also negative values of A are allowed we would obtain fixed points in the left-hand half-plane. Their stability can be considered as above. The corresponding stability regious we also given in fig. 3.2 as two further quarter turns of the shaded region at the positive x-axis.

The following observation shows that for $A > \sqrt{2}$ stability is only possible for a fixed point in a narrow strip just below the x-axis. It suffices to note that the line $x = 1/\sqrt{2}$ is tangent to the line $r^2 = \tan\theta$ at $\theta = \pi/4$.

4. Invariant manifolds

In the dissipative case which is considered here the attractor of the map (1.1) can be a finite set of stable fixed points or periodic points. If all those points are unstable the attractor may look like a so-called strange attractor. In [1] such an attractor is shown for the case $A = 3.9$, $B = 0.4$, $\beta = 0$. Here a similar illustration is given in fig. 4.1 for $A = 2$, $B = 0.6$, $\beta = 0$. A blow-up is given in fig. 4.2 showing a remarkable fine structure.

The attractor whether strange or not is an invariant set of the map and it may be obtained as a subset of

the unstable manifolds of the unstable fixed points which are all saddles. In this section we construct the unstable manifold S of a particular saddle. It is an analytic curve of the kind

$$x = F(t) \ , \ y = G(t) \ , \tag{4.1}$$

where F and G are entire functions of t so that S is an analytically smooth curve. It is shown that S has the desired appearance of a spiral with an infinite number of hairpin bends (cf. fig. 4.3).

The map transports a point with parameter t of S along the manifold into the point of S with parameter λt where λ is the unstable multiplier of the corresponding fixed point. The general situation is roughly that points not on S are attracted to S by the factor λ' where λ' is the stable multiplier - note that $\lambda\lambda' = B^2$ - and are displaced parallel to S by the factor λ.

A simple geometrical argument shows that the attractor of the map is always bounded. In section 1 we have seen that the map is the product of a rotation with contraction R and a translation T. This shows that an arbitrary disk $|z| < \rho$ is transformed into the disk $|z-A| < B\rho$. However, this disk is inside the disk $|z| < B\rho+A$. The transformation

$$\rho \rightarrow B\rho + A$$

defines a linear iterative process. Since $B < 1$ it converges to the limit $\rho_\infty = A/(1-B)$. Thus the attractor will be inside the closed disk

$$|z| \leqslant A/(1-B).$$

If the map is applied once again we see that the attractor is in the closed disk

$$|z-A| \leqslant AB/(1-B). \tag{4.2}$$

This result is important enough to state it as a theorem.

Theorem *The attractor of the dissipative map is contained in the closed disk (4.2).*

In order to construct the unstable manifold at the unstable fixed point z_0 we write

$$z = z_0 + F(t) \tag{4.3}$$

where

$$F(t) = \sum_{k=1}^{\infty} c_k t^k \tag{4.4}$$

with complex coefficients c_k and a real parameter t. The action of the map (1.1) is as

$$z_0 + F(t) \rightarrow z_0 + F(\lambda t)$$

where λ is the unstable multiplier. This gives the functional equation.

$$F(\lambda t) = B(z_0+F(t))\exp i\ (|z_0+F(t)|^2-\beta) - Bz_0 \exp i\ (|z_0|^2-\beta). \tag{4.5}$$

Both sides of (4.5) can be expanded as a Taylor series. Equating equal power of t we obtain relation of the following kind

$$\Phi(c_k \ , \bar{c}_k \ , \lambda^k) = \Psi_k(c_1, \bar{c}_1, c_2, \bar{c}_2, \ldots, \bar{c}_{k-1}) \tag{4.6}$$

for $k = 1,2,...$, where

$$\Phi(c, \bar{c}, \lambda) = (\lambda \exp i\ (\beta - r^2) - B(1+ir^2))c - iBz^2\bar{c} \ , \tag{4.7}$$

with $z = z_0$, $r^2 = |z_0|^2$.
For $k = 1$ we have $\Psi_k \equiv 0$. Then (4.6) and its complex conjugate are equivalent to the eigen vector equations at z_0. The eigenvalue equation obtained by eliminating c and c' determines the multipliers of z_0

$$\lambda^2 - 2B\lambda Re((1-ir^2)\exp i\ (\beta - r^2)) + B^2 = 0. \tag{4.8}$$

If λ is the multiplier with the largest absolute value the coefficients c_1 and $\bar{c}_1$ are determined up to an arbitrary common multiplicative constant. This is no disadvantage since t is still free. All further coefficients can be determined unqiuely from (4.6) and the complex conjugate equation. Solving these with respect to c_k and c_k' we obtain expressions of the kind

$$(\lambda^{2k} - S\lambda^k + B^2)c_k = ... \tag{4.9}$$

where $\lambda^2 - s\lambda + B^2 = 0$ is the eigenvalue equation (4.8). This means that $s = \lambda + \lambda'$ so that $\lambda^{2k} - s\lambda^k + B^2 = (\lambda^k - \lambda)(\lambda^k - \lambda')$.

Appendix Description of figures

Fig. 1.1 Spiral-structure in the dissipative case $A = 0.5$; $B = 0.99$; $\beta = 0$; Start : (1,1) ; scale: -1, 2, -0.5, Stationary point : (0.2625, 0.7552)

Fig. 1.2 Six orbits in the Hamiltonian case $A = 0.5$; $B = 1$; $\beta = 0$; scale: -1.5, 2.5 -1.1667 Stationary point: (0.25, 0.7580)

Fig. 2.2 Graphical method for determination of r^2 from a stationary point for eight values of A. $B = 0.6$; $\beta = 0$; scale -1, 30, -0.5 ,5

Fig. 2.3 Curves of equal (in) stability for same values of p; scale: -0.5, 4, -1, 2

Fig. 2.4 Construction of the two possible values of A (with B en β given)

Fig. 2.5 Meaning of the possible values of a stationary point

I : both stable

II : A - of fig. 2.4 is stable

III : Unstable

IV : A + of fig. 2.4 is stable

V : Unstable

Fig. 2.6 Regions of stability for some values of B as explained in fig. 2.5; scale: -0.5, 4, -1,2

Fig. 3.1 Regions of stability (shaded area) in the Hamiltonian case for $A >$; scale: -3, 6, -3, 3

Fig. 3.2 Same as fig. 3.1 plus the curve of the fixed point condition: $r = \sqrt{\beta \pm \pi - 2\theta}$ $B = 1$; $\beta = 0$; scale: -5, 10, 5, 5

Fig. 4.1 5,000 successive points of the strange attractor. $A = 2$;$B = 0.6$; $\beta = 0$; scale: -1, 8, -3, 3

Fig. 4.2 Blow-up of fig. 4.1; scale: 0.3, -0.5, 1.5

Fig. 4.3 Unstable invariant curve of one the seven stationary points stationary point : (3.96699, -1.67532) eigenvalue $\lambda = 7.79940$ $A = 2$; $B = 0.6$; $\beta = 0$; scale: -1, 8, -3, 3

Fig. 4.4 Compilation of figures 2.1, 2.3, 2.5 and the limit cycle of the attractor in the case $A = 2$; $B = 0.6$; $\beta = 0$; scale: -1, 8, -3, 3.

References

[1] K. IKEDA, H. DAIDO & O. AKIMOTO. Optical turbulence: Chaotic behaviour of transmitted light from a ring cavity. Phys. Rev. Lett. 45, 709-712 (1980).

[2]. J.V. MOLONEY Opt. Commun. (in press).

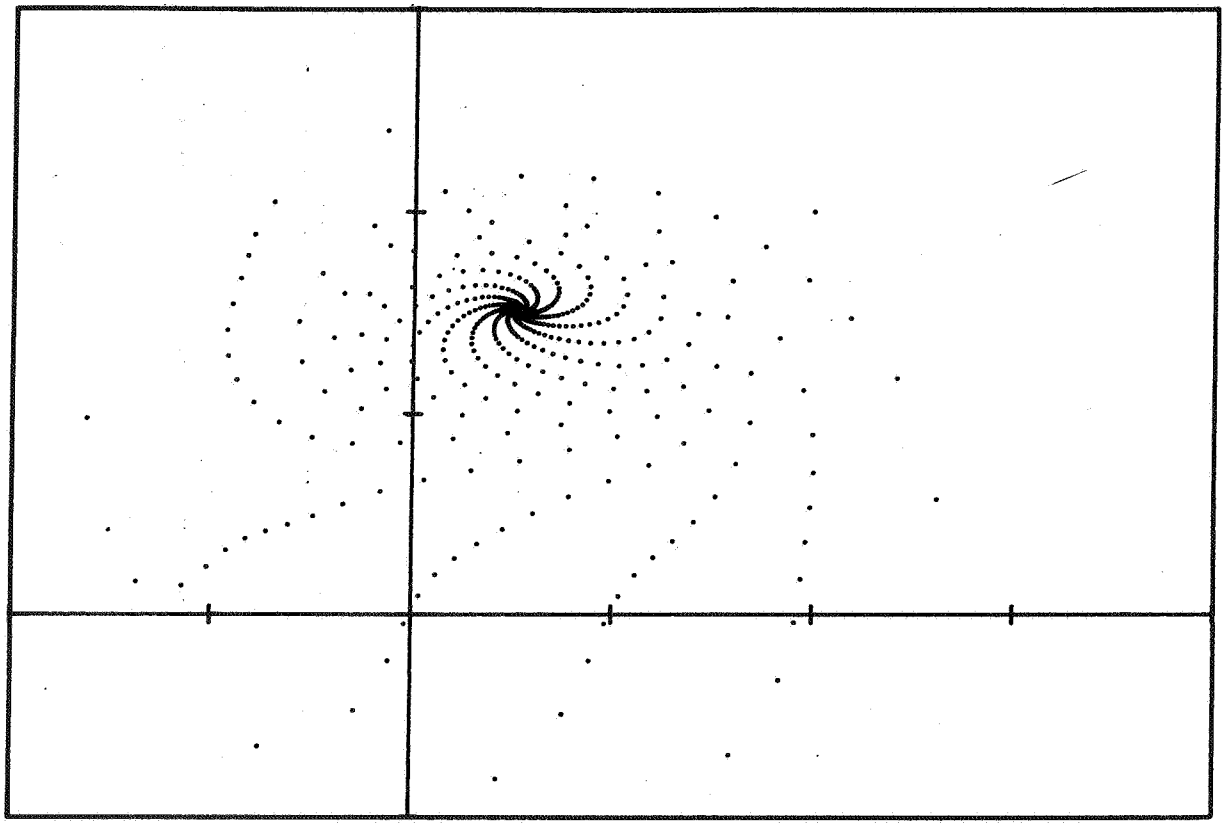

Fig. 1.1. Spiral structure in the dissipative case

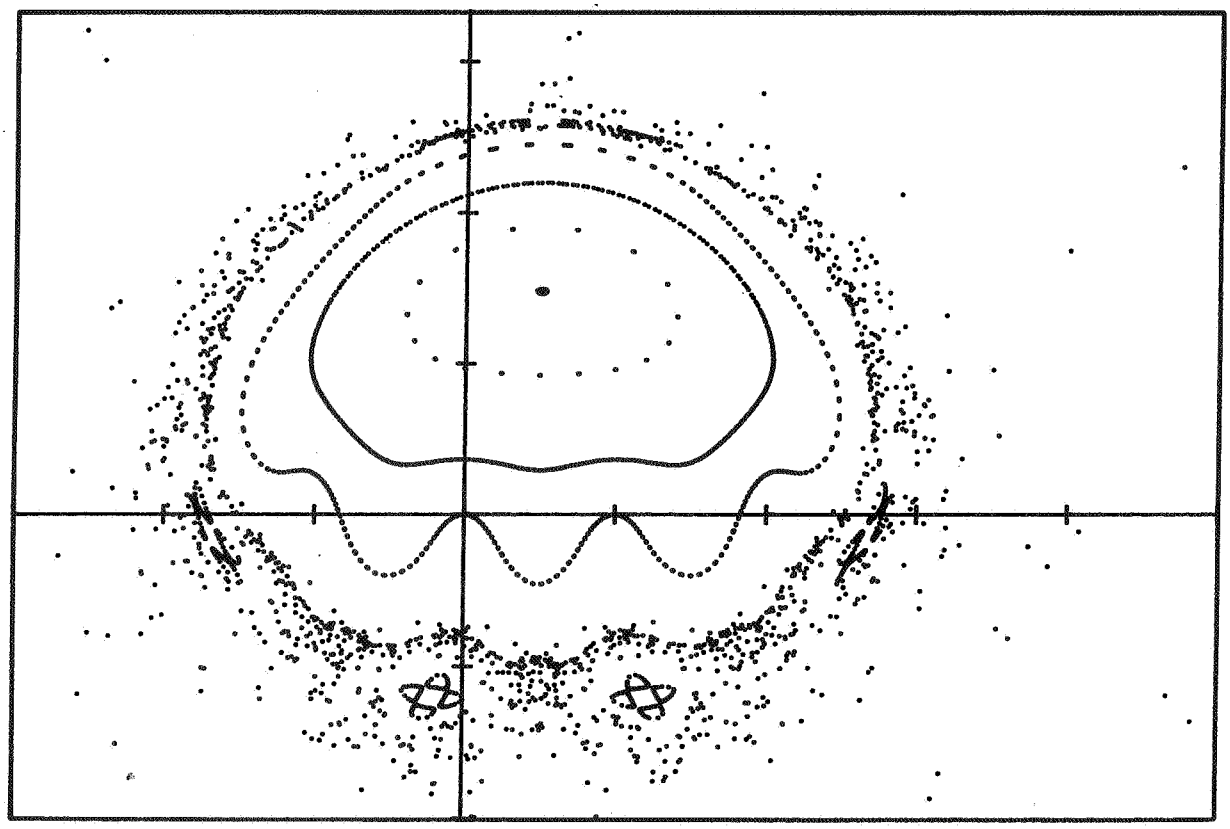

Fig. 1.2. Six orbits in the Hamiltonian case

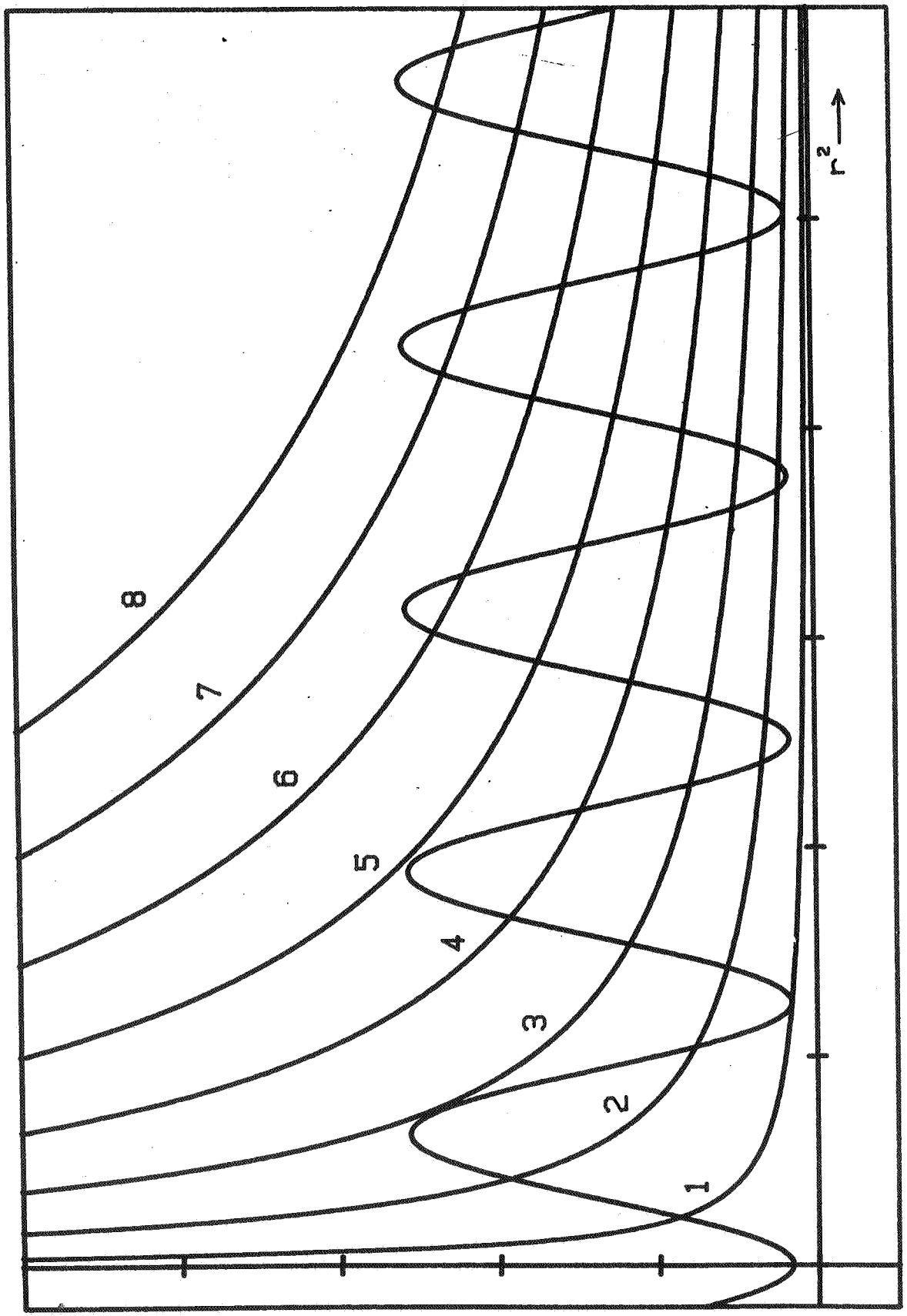

Fig. 2.2. Graphical determination of r^2 of a fixed point for eight values of A

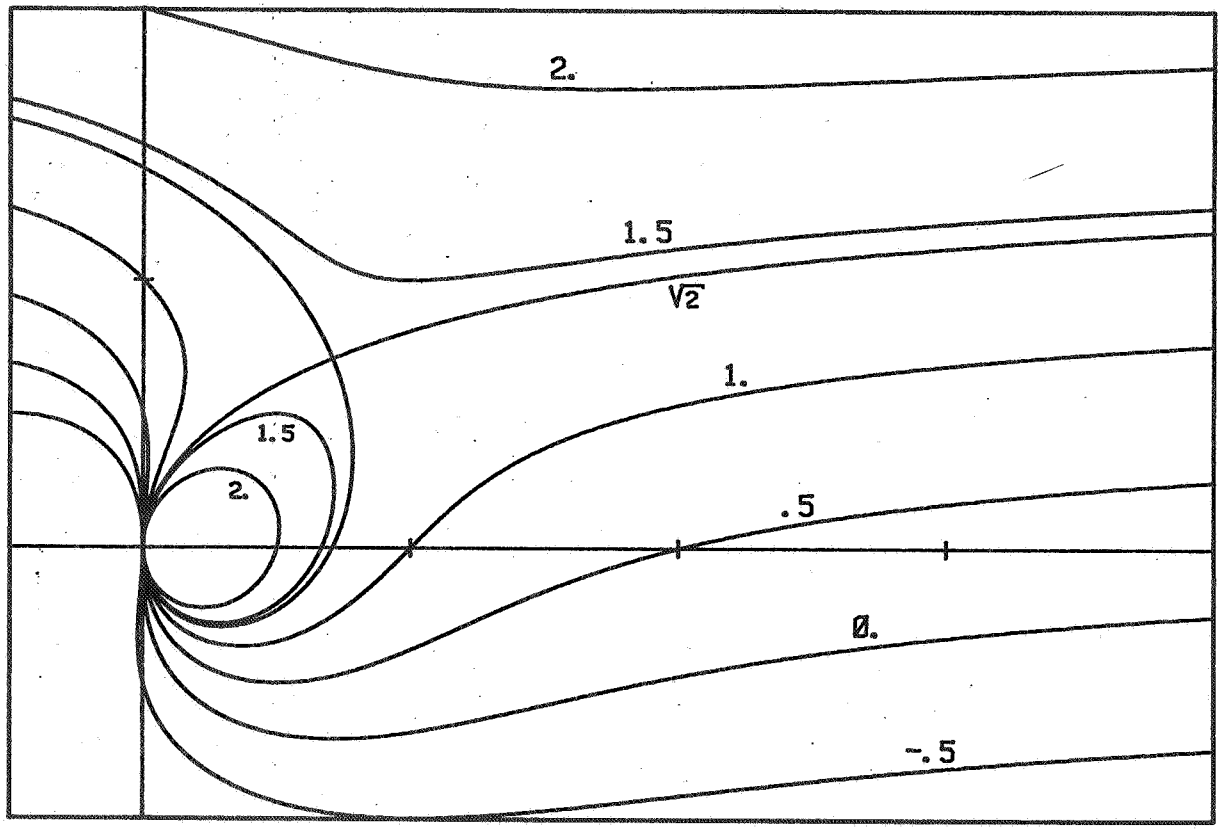

Fig. 2.3. Curves of equal (in) stability for some values of p

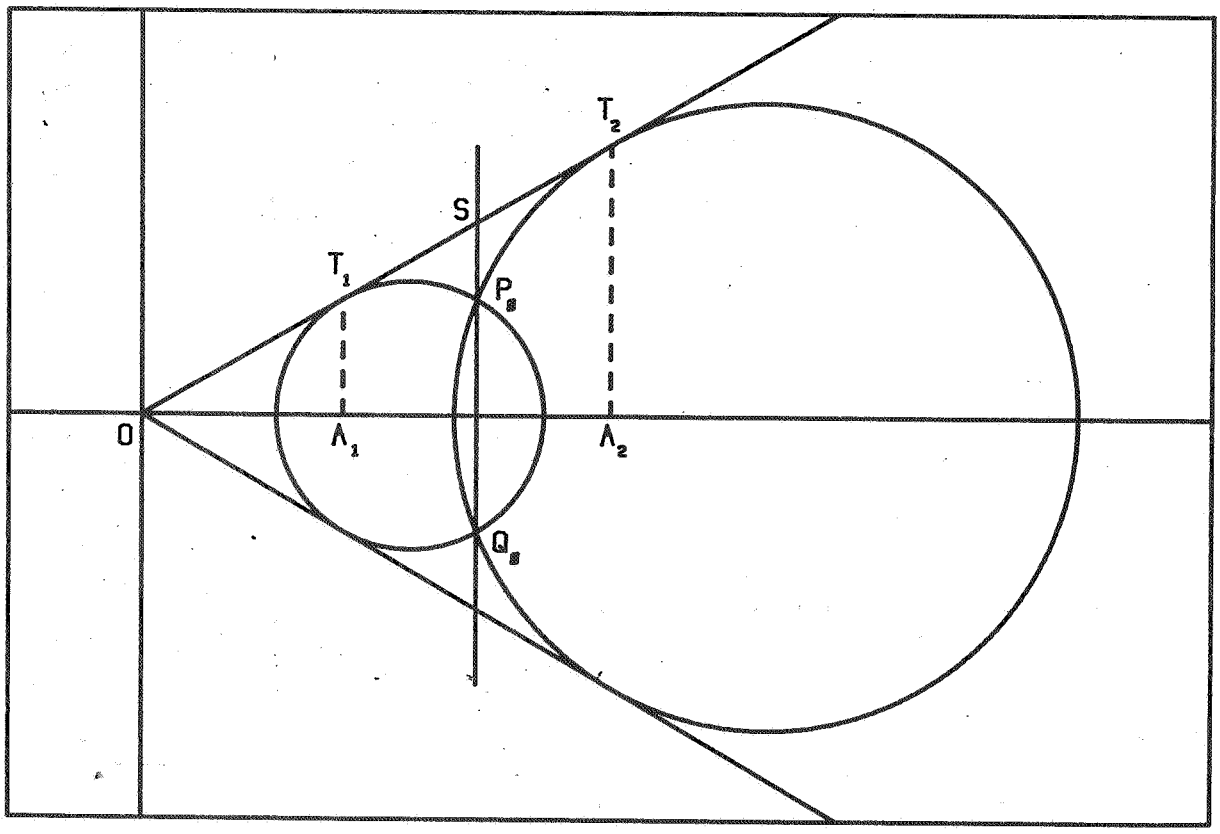

Fig. 2.4. Construction of the two possible values of A (with B and β given)

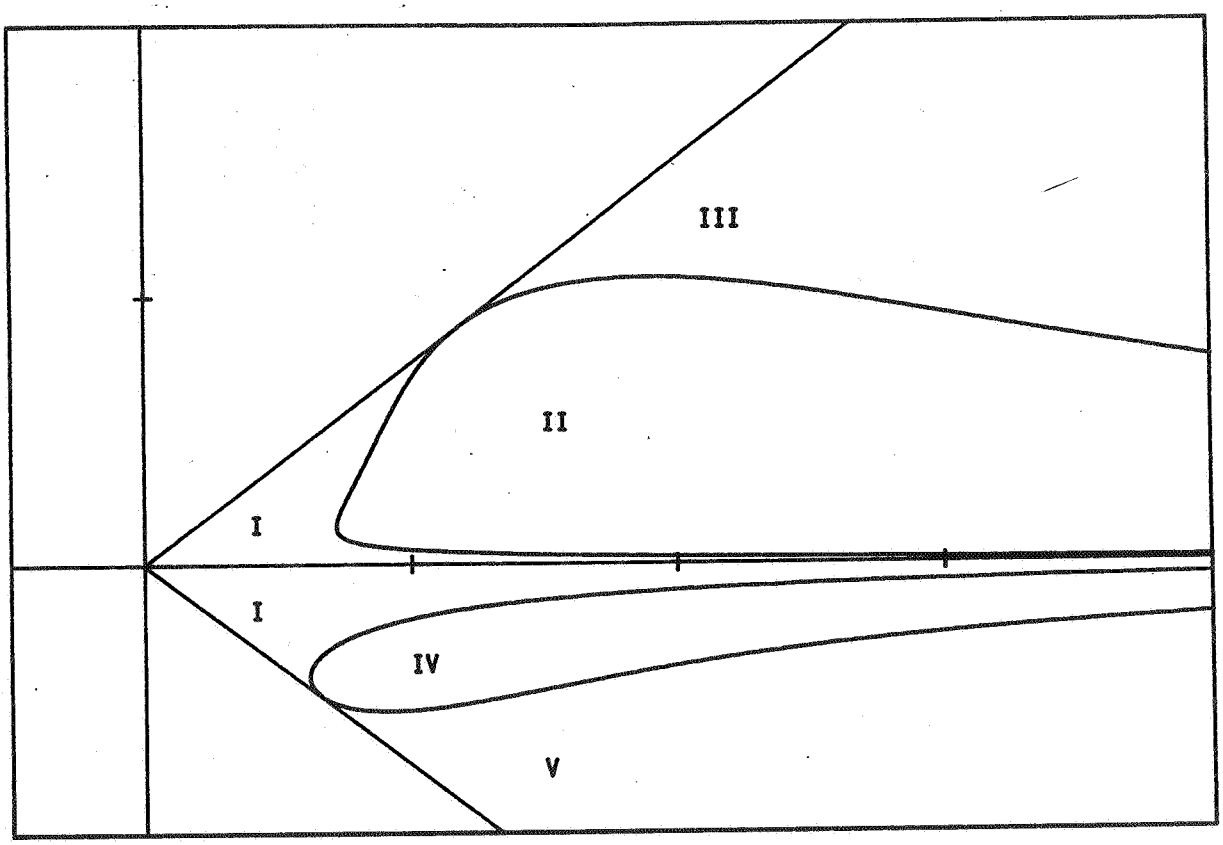

Fig. 2.5. Meaning of the possible regions of stabilityof a fixed point

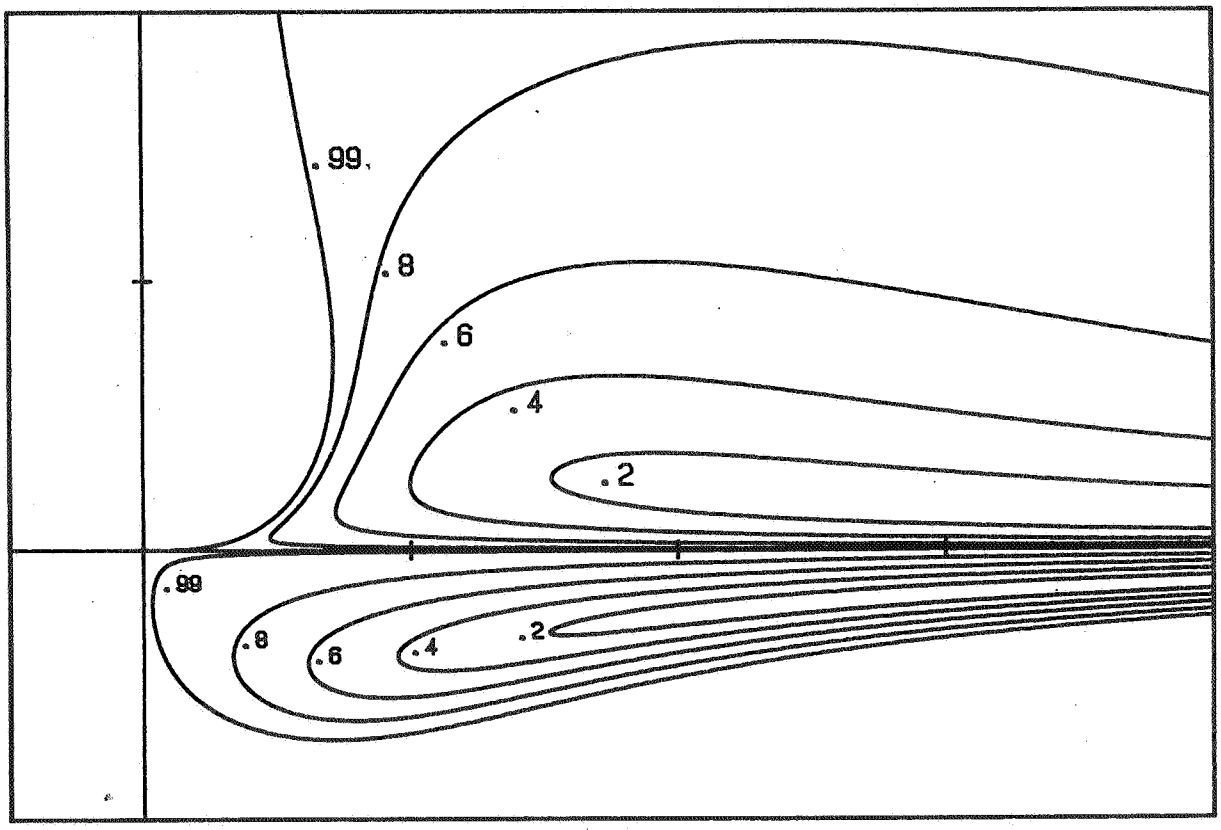

Fig. 2.6. Regions of stability for some values of B as explained for fig. 2.5

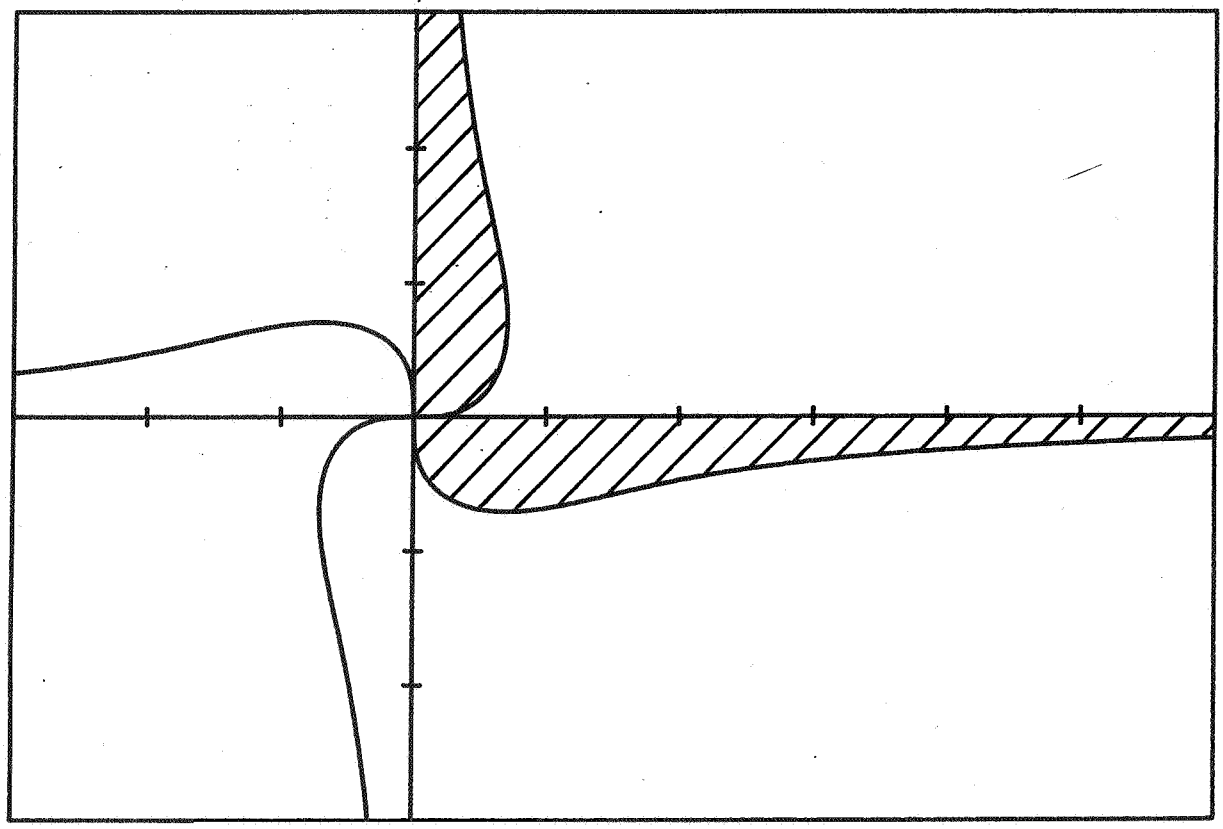

Fig. 3.1. Regions of stability (shaded) in the Hamiltonian case for $A > 0$

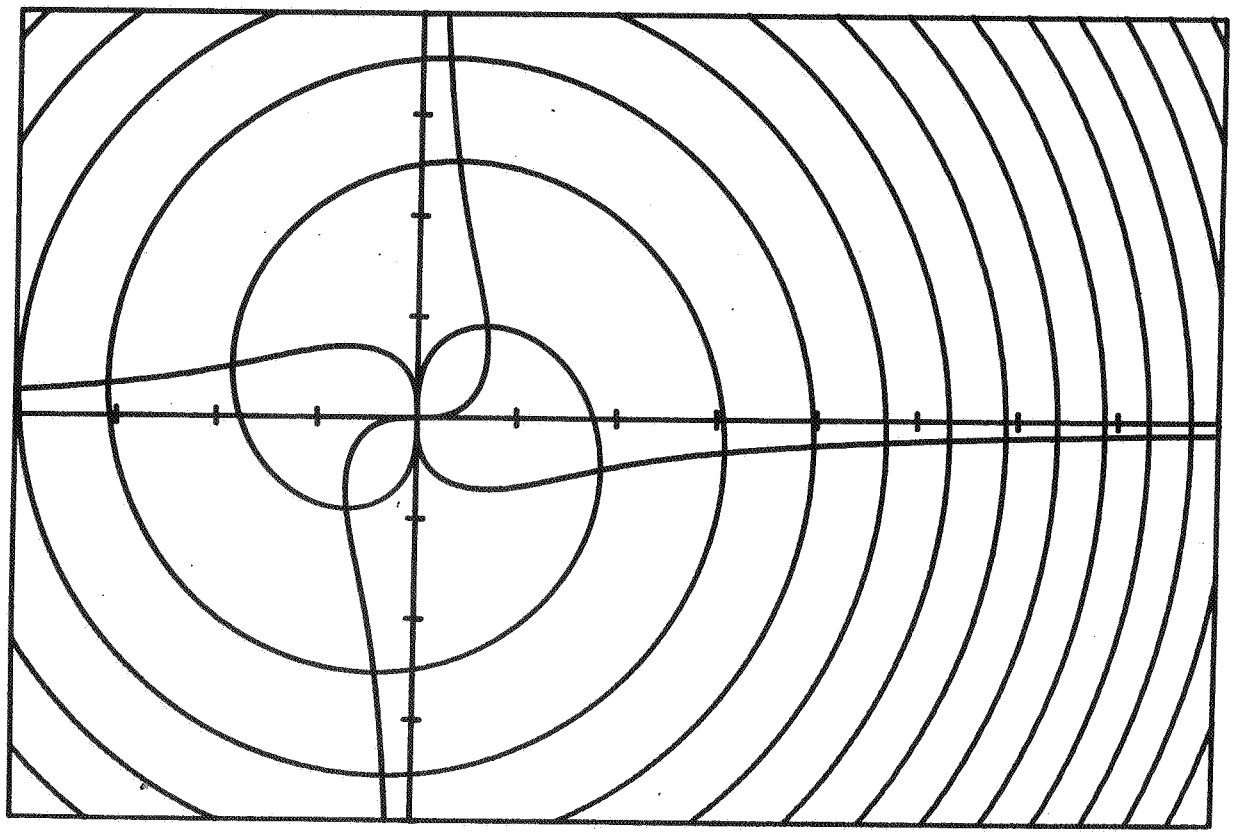

Fig. 3.2. Compilation of fig. 3.1 and the curve of the fixed point condition $r = \sqrt{\beta \pm \pi + 2\eta}$

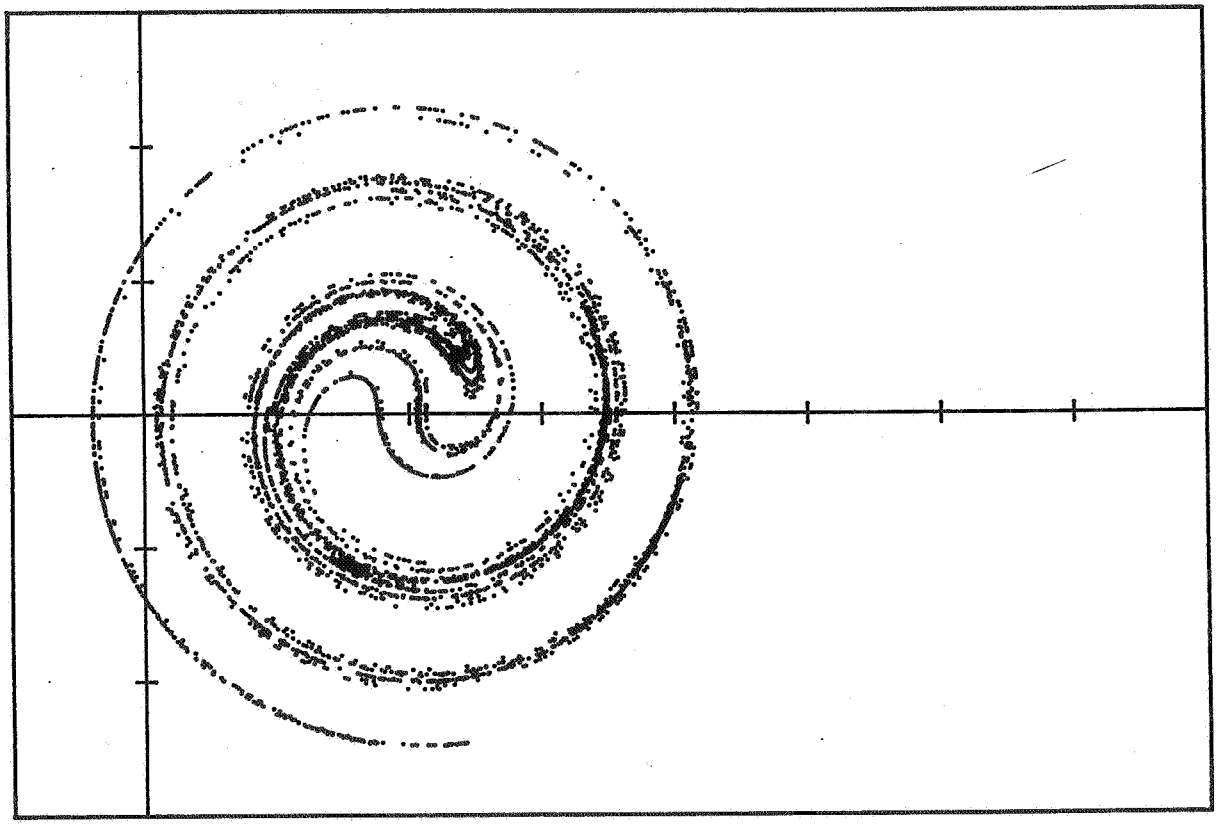

Fig. 4.1. 5000 successive points of the strange attractor

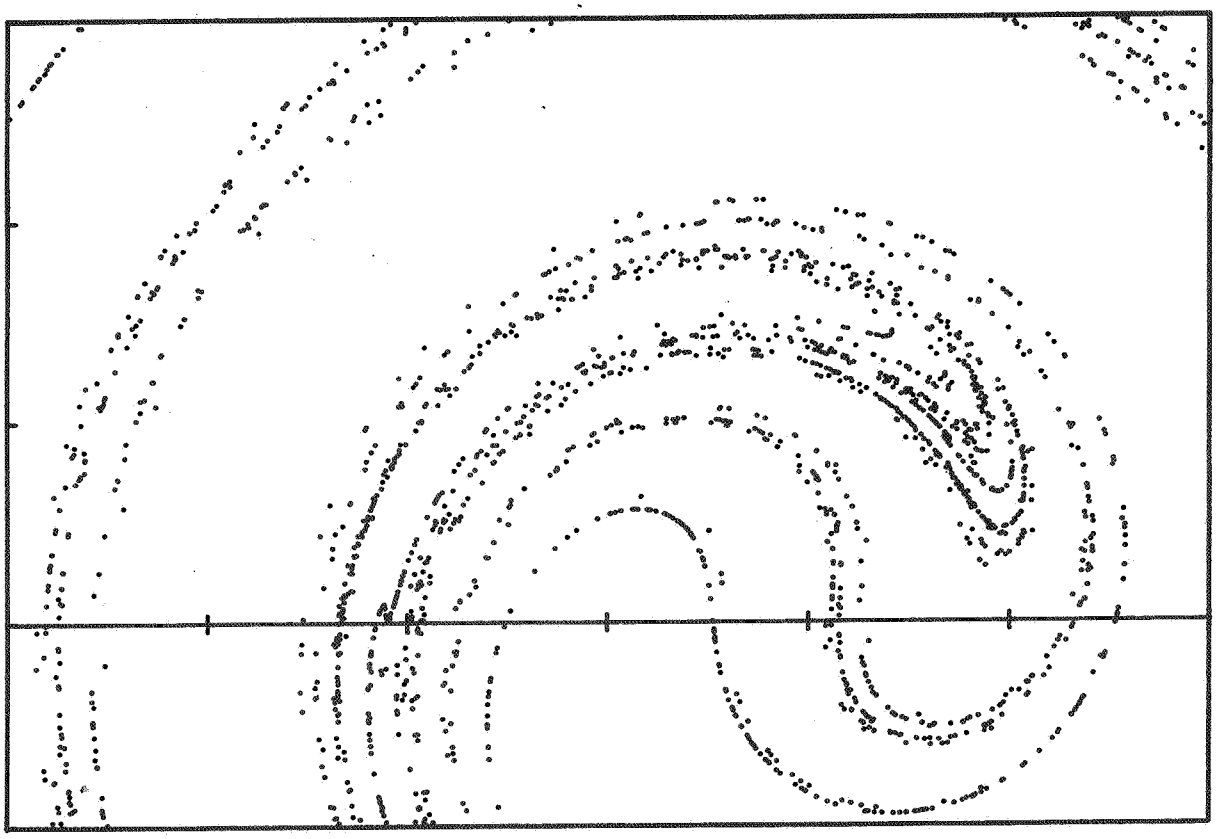

Fig. 4.2. Blowup of fig. 4.1

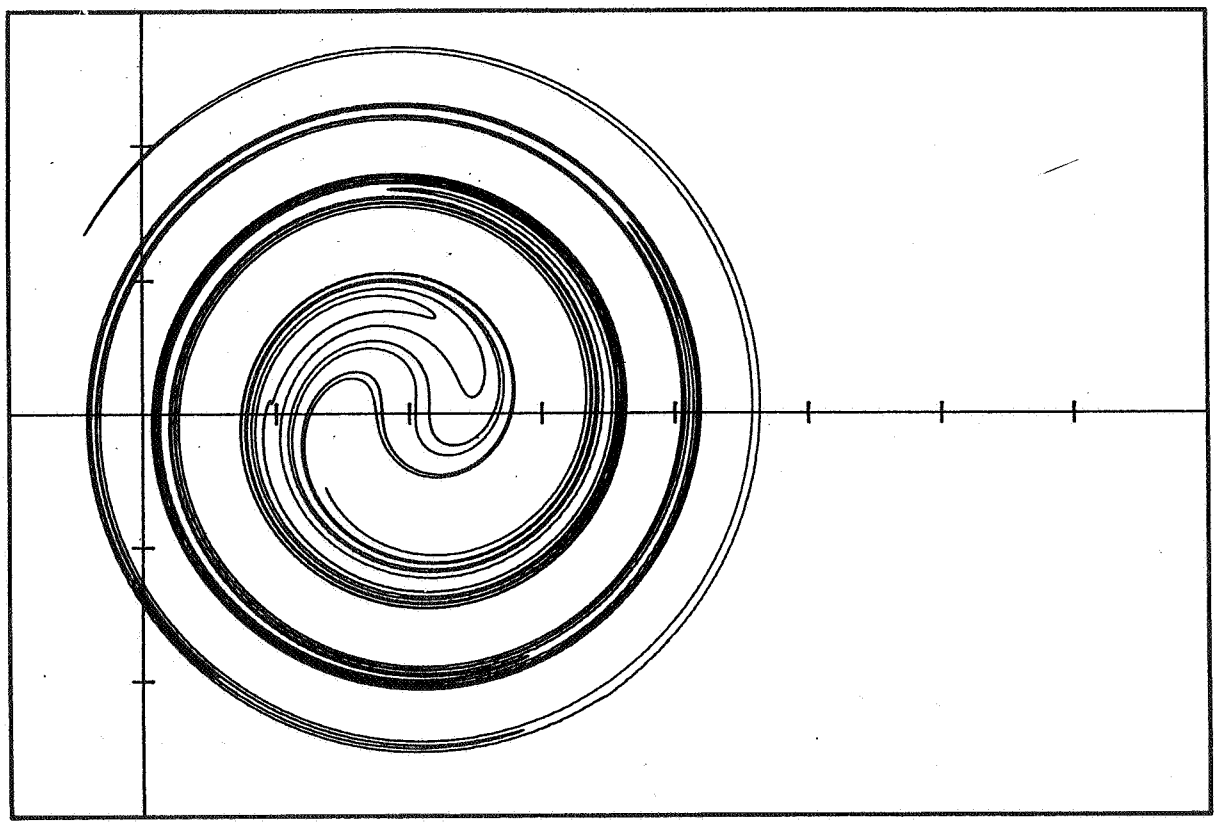

Fig. 4.3. Unstable invariant curve of one of the seven stationary points of 4.1

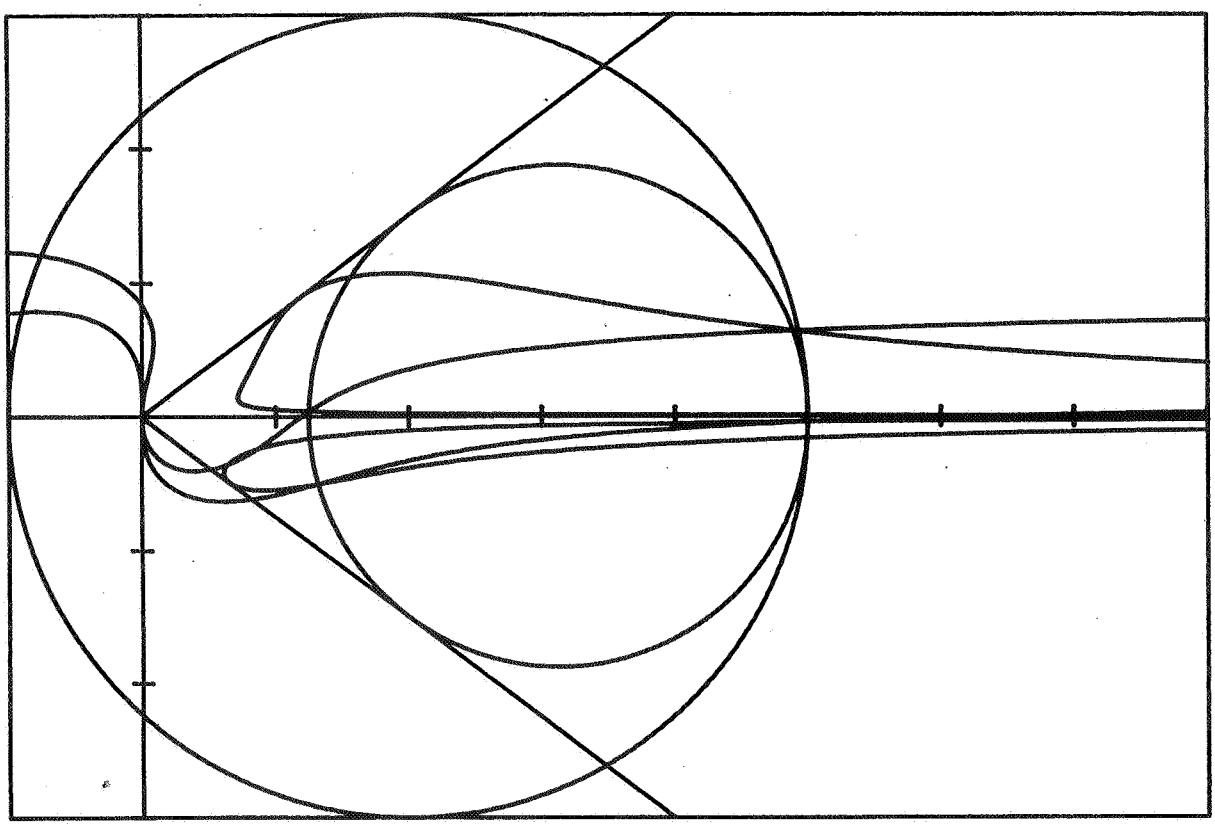

Fig. 4.4. Compilation of figures 2.1, 2.3, 2.5 and the limit of the attractor for fig. 4.1.